J Comput Aided Mol Des (2011) 25:1135–1145
DOI 10.1007/s10822-011-9498-x

Novel inhibitors to *Taenia solium* Cu/Zn superoxide dismutase identified by virtual screening

P. García-Gutiérrez · A. Landa-Piedra · A. Rodríguez-Romero · R. Parra-Unda · A. Rojo-Domínguez

Received: 21 April 2011 / Accepted: 21 November 2011 / Published online: 4 December 2011

Abstract We describe in this work a successful virtual screening and experimental testing aimed to the identification of novel inhibitors of superoxide dismutase of the worm *Taenia solium* (*Ts*Cu/Zn–SOD), a human parasite. Conformers from LeadQuest® database of drug-like compounds were selected and then docked on the surface of *Ts*Cu/Zn–SOD. Results were screened looking for ligand contacts with receptor side-chains not conserved in the human homologue, with a subsequent development of a score optimization by a set of energy minimization steps, aimed to identify lead compounds for in vitro experiments. Six out of fifty experimentally tested compounds showed μM inhibitory activity toward *Ts*Cu/Zn–SOD. Two of them showed species selectivity since did not inhibit the homologous human enzyme when assayed in vitro.

Keywords Taenia solium · Superoxide dismutase · Cu/Zn–SOD · Neurocysticercosis · Inhibition · Docking · Molecular operating environment, MOE

Introduction

Cysticercosis is a parasitic disease caused by infection with the larval stage of *Taenia solium* which occurs when humans become the intermediate host in the life cycle of the helminth [1]. The parasite infects the central nervous system thus producing neurocysticercosis (NCC), considered the most common parasitic disease of the CNS and affects millions of people in developing countries of Latin America, Africa and Asia, as well as in developed countries with a high migration ratio of subjects from endemic areas [2–4]. This condition is associated with severe neurological manifestations including epilepsy, headaches, seizures and other neurological disorders [5]. Conservative estimates describe 50,000 deaths worldwide every year due to neurocysticercosis [6]. The treatment for NCC in humans is based on two drugs: albendazole and praziquantel. Both drugs can cause adverse symptoms in the host, but in general are well tolerated. These drugs are often administered with dexamethasone to decrease the inflammatory reaction produced by the host in response to the death of the parasite, a reaction that some times can also kill the host [7]. To date, there is only one report on drug-resistance to praziquantel and albendazole in Cestode infections found in a patient with neurocysticercosis [8], but resistance to these and other drugs has been reported

Electronic supplementary material The online version of this article (doi:10.1007/s10822-011-9498-x) contains supplementary material, which is available to authorized users.

P. García-Gutiérrez · A. Rojo-Domínguez
Área de Biofisicoquímica, Departamento de Química, Universidad Autónoma Metropolitana–Iztapalapa, 09340 México, D.F., México
e-mail: pgarcia@ciencias.unam.mx

A. Landa-Piedra · R. Parra-Unda
Departamento de Microbiología y Parasitología, Facultad de Medicina, Universidad Nacional Autónoma de México, 04510 México, D.F., México

A. Rodríguez-Romero
Departamento de Biomacromoléculas, Instituto de Química, Universidad Nacional Autónoma de México, 04510 México, D.F., México

A. Rojo-Domínguez (✉)
Departamento de Ciencias Naturales, Universidad Autónoma Metropolitana–Cuajimalpa, Pedro A. de los Santos 84, Col. San Miguel Chapultepec, 01120 México, D.F., México
e-mail: arojo@correo.cua.uam.mx

for other helminths such as schistosomes and some nematodes [9, 10]. Therefore, there is an urgent need to develop new drugs with different mechanisms of action.

Superoxide dismutases (SODs) are a group of metalloenzymes essential for defending organisms against oxidation by the superoxide anion ($O_2^{\cdot-}$) [11, 12]. SODs catalyze in two steps the dismutation of the $O_2^{\cdot-}$ to molecular oxygen and hydrogen peroxide. Although $O_2^{\cdot-}$ is a mild reductant, it can cause direct or indirect damage to cell membranes and DNA [13]. Three major classes of SODs have been described on the basis of their prosthetic groups: Fe, Mn, or Cu/Zn. So far, three types of SOD enzymes have been identified in helminths: the mitochondrial Mn–SOD, the cytosolic and an extracellular Cu/Zn–SOD [14, 15]. Organisms lacking these enzymes exhibit a decreased growth rate, shorter life span, hypersensitivity towards redox cycling compounds such as paraquat and quinones, and an increment in spontaneous mutagenesis and death rates [11, 12]. As a other parasitic organisms, *T. solium* must remove endogenous and exogenous $O_2^{\cdot-}$ produced by its own metabolic processes and, because its larval and adult stages live in tissues, the one produced by host inflammatory response [16].

As reported by some authors [9], albendazole inhibits microtubule formation in parasite by binding to β-tubulin, however, as shown by Sánchez-Moreno et al. [17–19], this drug also inhibits SOD enzymes in helmints, but at high concentrations in the case of *T. solium*, as reported by us [20]. Gómez-Contreras et al. [21] reported recently the synthesis of benzo[*g*]phthalazine derivatives which selectively inhibit Fe–SOD activity and growth of *Trypanosoma cruzi*. Beznidasole, a drug currently used against trypanosomiasis act trough inducing formation of toxic oxygen metabolites such as superoxide anion and hydrogen peroxide [22].

These and other reports suggest that SOD enzymes are involved in parasite defense [15]. Our hypothesis is that inactivation of this enzyme may contribute to weaken the defense mechanisms of the parasite and aid destroying it, thus SOD can be considered a good target for drug design.

Recently, we resolved the crystal structure of recombinant *Ts*Cu/Zn–SOD at 2.7 Å resolution, an homodimer with 152 residues and one Cu and one Zn atom per active site by monomer (PDB entry 3MND) [23]. It possesses the classical motifs of Cu/Zn–SOD enzymes. All residues directly or indirectly involved in metal binding are completely conserved. Nevertheless an analysis comparing the amino acid sequence of *Ts*Cu/Zn–SOD with other SODs reported in databases, showed low global identity of 57.2, 57.9 and 59.6% with mammals such as *Sus scrofa* (pig), *Homo sapiens* (human) and *Bos taurus* (bovine), respectively, suggesting that differences in *Ts*Cu/Zn–SOD can be used to design specific inhibitors.

Materials and methods

Molecular modeling, electric partial-charge assignation, ligand conformer, searching of potential binding sites, energy minimizations, visualization and docking were performed with molecular operating environment (MOE) [24] package with default parameters, unless otherwise stated. Energy minimizations were carried out until an RMSD (root mean square deviation) force lower than 0.001 was obtained using CHARMM27, an all-atom force field parameterized for proteins, or MMFF94x, parameterized for small organic molecules in medicinal chemistry.

Generation of 3D conformers from LeadQuest® database

Exelgen LeadQuest® database [25] was used as the initial chemical space for this study. Each of the 51,068 compounds was prefiltered using Lipinski-like rules as follows: molecular weight <600, LogP <7, donors + acceptors <12, rotatable bonds <7, and transformed into 3D molecular structures using *Import_Database–MOE*. Then, we generated a chemically diverse 3D conformational database of drug-like molecules with *Conformer_Import–MOE*, using a cut-off conformational energy of 3 kcal/mol from the minimum energy structure of each compound, as calculated with the MMFF94x force field. The adopted procedure allowed the generation of a chemically diverse 3D conformational database of multiple conformers for each molecule, which was then used for docking. The X-ray structure of *Ts*Cu/Zn–SOD and human Cu/Zn–SOD (*Hs*Cu/Zn–SOD, PDB entry **2V0A**) were used as protein targets for docking procedures.

Potential binding sites were identified with the *Site_Finder–MOE* and with CASTp server [26]. All crystallographic water molecules were removed from the protein structures before docking. Hydrogen atoms and partial charges were added to the enzyme using the CHARMM27 force field. Charge for Cu and Zn was set to 2^+. *Dock–MOE* studies used the alpha-site-triangle method [27] to bias the orientation search of the ligand to meaningful trials, and the docking score function named *Affinity dG* was used as implemented in MOE [28]. GW572016 (Lapatinib) is a tyrosine kinase inhibitor that is a potent dual inhibitor of epidermal growth factor receptor (EGFR, ErbB-1) and ErbB-2. X-ray structure of EGFR bound to GW572016 was well resolved and published [29]. That complex (PDB entry 1XKK) was used as a docking validation. Docking score found with MOE was −11.3, with a root mean square deviation of the pose from the original ligand of 1.93 Å.

Docking on *Ts*Cu/Zn–SOD X-ray structure

In a first screening, 15,000 orientations or poses on potential binding sites were proved and evaluated for each conformer from each compound in the 3D conformational database; the top ten scoring poses for each conformer were written out to a new database [30]. In a second step, conformers of compounds with good scores (docking scores <-7.5 units) were resubmitted for evaluation, but allowing in this case the search of 100,000 poses. Only those compounds for which the top scoring energies achieve values lower than -8.6 were selected for further analysis. Energy minimization of the best and/or the most frequently found docked poses for each compound was carried out to refine the orientation of the ligand in the receptor site, and to find the local energy minimum of the ligand–enzyme interactions. Three protocols were designed for optimizing the ligand–enzyme complexes. In method 1, the receptor was treated as a rigid structure and the ligand was allowed to relax into the active site. For method 2, residues of the active site ($\leq$4.5 Å) and the inhibitor were allowed to relax while the rest of the receptor were fixed; 3. Finally, in method 3 all residues at 4.5 Å from the ligand were subjected to an energy minimization with the coordinates of the ligand fixed, then only the ligand was relaxed with the fixed new positions of the nearby residues; and finally new energy minimization of contact residues was carried out, again with the ligand fixed. This latter method was the most efficient in further lowering the ligand–enzyme energy interaction.

After visual inspection of the minimized protein–compound complex, a set of compounds were selected for in vitro testing of their inhibitory potency against pure recombinant *Ts*Cu/Zn–SOD and commercial *Hs*Cu/Zn–SOD (Sigma) on basis of several criteria: we searched for ligand binding contacts to non-conserved side chains of the enzyme, shape complementarily, docking score before minimizing energy of complex, predicted LogP less than 5.5, number of hydrogen bonds formed, among others (see Results and discussion for more details).

Compounds **1–6** were docked on *Hs*Cu/Zn–SOD X-ray structure with an extensive search of 100,000 poses of each conformer in order to determine their docking score and compare it with *Ts*Cu/Zn–SOD.

In order to compare docking scores from *Dock–MOE* for compounds **1–6**, we carried out an extensive docking procedure using alternative software. The *AutoDock–Vina* (*Vina*) software [31] was used for flexible docking simulations. The compounds **1–6** were docked into binding site 1 on *Ts*Cu/Zn–SOD surface. Before docking, water molecules were removed from the X-ray structure. Polar hydrogens and Gasteiger charges were assigned using the *AutoDock–Tools* interface [32]. Then, the size of search spaces in each dimension (x, y and z) for site 1 was $26 \times 26 \times 30$ Å with center in -10.784, 0.686 and -31.058; for site 2, dimensions are $24 \times 24 \times 24$ Å with center in -13.799, -1.323 and -1.359. The other *Vina* default optimization parameters were maintained for docking simulation. Docking scores for the best poses for compounds **1–6** according to *Vina* shown in Table 5 in Supplementary Material.

*Ts*Cu/Zn–SOD enzyme inhibition assays

Recombinant *Ts*Cu/Zn–SOD enzyme was expressed and purified as described previously [20]. Enzyme inactivation was determined indirectly by measuring inhibition of cytochrome *c* reduction caused by $O_2^{\cdot -}$, which is produced by the xanthine–xanthine-oxidase system [33]. The reaction was carried out in a final volume of 1.0 mL in the presence of 10 units of recombinant enzyme (specific activity 2,940 units/mg, 3.5 μg enzymes) incubated for 30 min at 37 °C with 100 μM of the selected LeadQuest® compounds [20]. One unit of SOD is defined as the amount of enzyme that causes 50% inhibition of the reduction of cytochrome *c* with incubation times of 2 min [33]. Only compounds with inhibitory activity (more than 30%) against *Ts*Cu/Zn–SOD were incubated against *Hs*Cu/Zn–SOD (Sigma, specific activity 4,000 units/mg). For those compounds with a percentage of inhibition of *Ts*Cu/Zn–SOD greater than the threshold of 60%, a complete set of measurements was performed to determine the IC_{50} values.

The tested compounds were purchased from Exelgen Inc. (formerly LeadQuest®). Purity reported by the manufacturer was greater than 95% checked by LC/MS. Stock solutions (10 mM) of each compound were made in DMSO, with similar aliquots of the pure solvent in blank experiments.

Results and discussion

Conformer search

MOE is a drug discovery package [24] used to perform several tasks in this work. In order to simulate ligand flexibility in our docking studies, we generated a set of low-energy conformers for each of the about fifty thousand compounds of the LeadQuest® database as described in the Materials and methods section. A high-throughput fragment-based conformational search [24] allowed the transformation of the original 51,068 compounds library into a new database of about 2 million conformers with energies $\leq$3.0 kcal/mol respects to the lowest minimum conformation of each compound. In this sense, Perola and Charifson [34] found that a 3.0 kcal/mol energy cut-off would retain

about 80% (50%) of bioactive ligands with 1–3 (4–6) rotatable bonds. For computational convenience we used this same threshold and accordingly we expect our conformational ensembles to contain a significant number of biologically relevant conformations. This new *in*-house database was then used for docking studies against the X-ray structure of *Ts*Cu/Zn–SOD.

Molecular docking

Before starting our docking calculations we determined potential sites for ligand binding from the 3D atomic coordinates of the *Ts*Cu/Zn–SOD. Active sites are usually hydrophobic pockets that involve side chain atoms tightly packed [35]; thus we searched for these sites on the

Table 1 Structure and biological activity of LeadQuest® compounds identified by virtual screening procedure that showed in vitro inhibition activity for *Ts*Cu/Zn–SOD

Compound	Structure	Best score against *Ts*Cu/Zn–SOD (and against the human homologue)	Preferred binding site according to best scores	*Ts*Cu/Zn–SOD IC_{50} (μM)
1	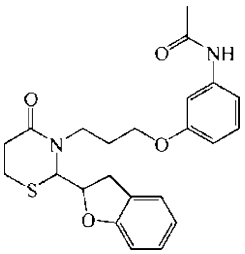	−8.6 (−5.5)	1	–[a]
2	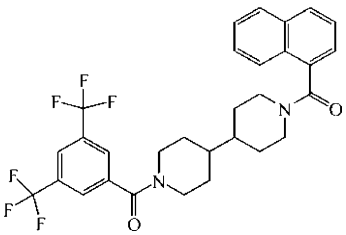	−8.7 (−6.0)	1, 2	23.9
3	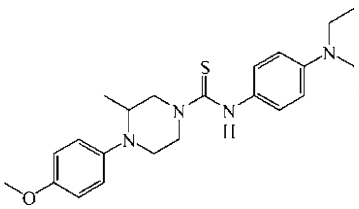	−8.8 (−6.1)	1	9.8
4	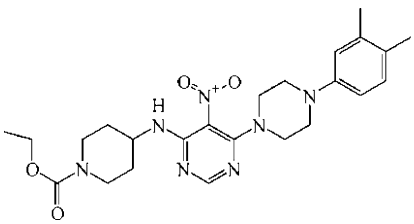	−9.0 (−6.0)	1	25.9
5	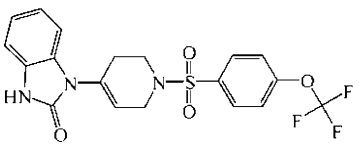	−9.0 (−6.3)	1, 2	–[a]
6	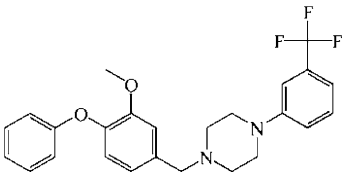	−8.7 (−5.9)	1, 2	–[a]

[a] IC_{50} values were only measured when the % inhibition was >60% at 100 μM of compound (see Materials and methods for more details)

molecule surface by filtering out sites with significant convex surfaces too exposed to solvent. The residues directly or indirectly involved in metal binding are conserved among the Cu/Zn–SODs from all species so far examined, from bacteria to mammals; therefore in order to attain species selectivity, the cavities from these sites were also discarded. On this basis, more than twenty potential sites were detected and distributed over the entire surface of the dimer, which were labeled as site 1, site 2, site 3, and so on (see Table 1 in Supplementary Material for the whole list and description). Sites 1 and 2 are the more prominent in size; they are located near the interface region and formed by atoms from 32 to 20 different residues, respectively, a reflection of their large site dimension. Site 1 and 2 are located in opposed parts of the dimer interface, so that potential binding sites are facing away from each other. Site 1 has an extended shape while site 2 is more compact one; both sites are rich in hydrophobic residues. Moreover, sites 1 and 2 are not strictly conserved between *Ts*Cu/Zn–SOD and *Hs*Cu/Zn–SOD sequences, which transform these sites in attractive targets for designing species-specific inhibitors. In contrast, the rest of the potential sites (3–22) are much smaller, exposed to solvent, and in many cases, well conserved respect to the human enzyme.

In a first stage, the previously generated conformers for each ligand were scanned against all sites on the *Ts*Cu/Zn–SOD surface, using 15,000 poses of probe for each conformer. We noticed that sites 1 and 2 always presented the highest docking scores while other sites always showed lower scores; therefore in the subsequent step, ligands with docking scores better than −7.5 (*c.a.* 500 different compounds) were re-scanned only on sites 1 and 2, but now with 100,000 poses of each conformer in order to include virtually all orientations for binding each of those compounds. This procedure yielded complexes with much better docking scores, those whose docking scores were better than −8.6 were then submitted to an energy minimization process in order to improve the interactions at the binding sites. This optimization process was carefully designed testing and evaluating different schemes of partial minimizations of the structure of the complexes (see Materials and methods for more details). We found a procedure aimed to find a better positioning of the ligands into the binding site, as judged from lowering the previously obtained ligand–enzyme energy interaction. This procedure consist in (1) first all residues at 4.5 Å from the ligand were subjected to an energy minimization with the coordinates of the ligand fixed, (2) then only the ligand was relaxed with the fixed new positions of the nearby residues, and finally (3) a new energy minimization of contact residues was carried out, again with the ligand fixed. This 3-step methodology optimized the protein–ligand contacts by allowing a better rearrangement of the side chains of the binding site and the position of the ligand as is reflected in the potential energy of the protein–ligand contacts (see Table 4 in Supplementary Material for more information).

Overall, the search for conformers and binding energy in three steps used in this work intended to include part of the conformational response of the enzyme due to the presence of the ligand in its binding site. From our results, a set of fifty compounds were selected to be tested in vitro against recombinant pure *Ts*Cu/Zn–SOD enzyme. The final compound selection which yielded the set of 50 compounds, included a final screening from the highest scored ligands identified by docking, it also included considerations of docking score, ligand–enzyme energy interaction, hydrophilicity, selectivity, molecular weight and robustness of prediction. Since it is our experience that hydrophobic compounds aggregate when dissolved from DMSO stock solution into aqueous inhibition tests, we privileged hydrophilicity in the final selection process. With respect to selectivity we gave preference to compounds forming contacts (e.g. hydrogen bonds) to non-conserved side chains of the receptor, to gain selective inhibition to

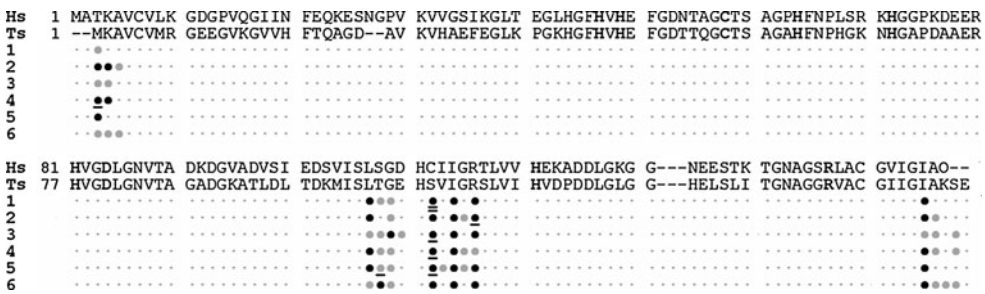

Fig. 1 *Ts*Cu/Zn–SOD and *Hs*Cu/Zn–SOD sequence alignment. Several (identity: 57.9%) residues are not conserved between sequences. Residues in contact (≤4.5 Å) with ligands **1**–**6** at site 1 on the *Ts*Cu/Zn–SOD surface are indicated by *circles*. *Black color* indicates that the ligand interacts with the residues in the chains **A** and **B**; *gray color* indicates that the ligand interacts with the residue only in one chain. Intrachain disulphide cysteine residues, conserved residues in the active site, and involved in Cu and Zn binding are in *bold letters*. *Lines* bellow the *circles* indicate the number of hydrogen bonds between ligand and residues, see Figure 1 in Supplementary Material for more details

parasitic SOD with respect to the human enzyme. In this respect, Fig. 1 shows *Ts*Cu/Zn–SOD and *Hs*Cu/Zn–SOD sequence alignment (identity: 57.9%). Residues in contact with ligands **1**–**6** at site 1 on the *Ts*Cu/Zn–SOD surface, according to our docking results, are indicated by circles: several residues present only in *Ts*Cu/Zn–SOD interact with **1**–**6** through hydrogen bonds. Finally, with robustness we mean the frequent finding of slightly different poses of the same compound with high scores, which means that small changes in orientation still yield a good predicted docking score. In addition, we also included ten compounds with medium and low docking score to use them as negative controls (structures, identifications and scores for all compounds used are depicted in Tables 2 and 3 in Supplementary Material). This includes compounds with low affinity for sites 1 and 2 and some of the best ligands for other binding sites. All candidate compounds were first evaluated for their ability to inhibit the activity of *Ts*Cu/Zn–SOD at 100 μM: six of the fifty tested compounds demonstrated >30% inhibition of the enzyme at μM concentrations. Table 1 and Fig. 2 show the structures of active compounds (**1**–**6**), and the residual activity of recombinant *Ts*CuZn–SOD obtained after incubation with 100 μM of these compounds, respectively. Examination of these active compounds revealed a diversity of chemical structures, they have molecular weights between 430 and 560 Da, estimated LogP [36] lower than 5.5, no more than 10 H-bond acceptors and a low flexibility. A common structural feature present in compounds **3**, **4** and **5** is a piperazine group. Three other chemical classes are constituted by sulfonamide, bipiperidinyl and acetanisidide derivatives. Clearly, their inhibitory capacity comes from their tight fitting to the binding site more than being variations or derivatives from a common structure. Six real in vitro hits out of fifty putative inhibitors represent an experimental-hit ratio of 12% [(6/50) × 100], which demonstrates the success of the virtual screening procedure. The rest of the tested compounds, including the negative controls, yielded very low or no inhibition and were considered as inactive. The aim of this work was to find agents that selectively inactivate *Ts*Cu/Zn–SOD. Therefore, in order to determine the docking scores of compounds **1**–**6** to *Hs*Cu/Zn–SOD we carried out an extensive docking procedure on the surface of this human enzyme. We found that the docking scores were always lower for the human enzyme than for the *T. solium* SOD, in good agreement with our experimental results: the best score occurs when compound **5** binds to site 2 with a docking score equal to −5.5.

Finally, we found that the *Vina* docking scores and poses for compounds **1**–**6** over site 1 on *Ts*Cu/Zn–SOD were in good agreement with *Dock–MOE* results (see Table 5 in Supplementary Material).

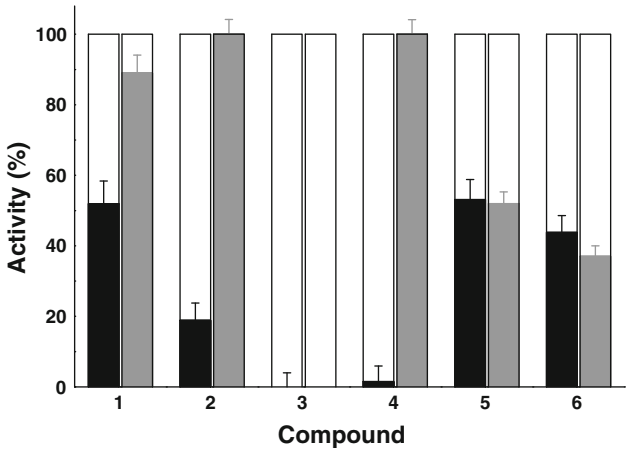

Fig. 2 Inhibition of *T. solium* and human Cu/Zn–SOD activity by incubation with active LeadQuest® compounds, determined by xantine–xantine-oxidase method. *T. solium* (*black bars*; 10 Units, 3.5 μg enzymes) and human Cu/Zn–SOD (*grey bars*; 10 Units) were incubated in presence of 100 μM for 30 min at 35 °C of compounds: **1**, **2**, **3**, **5** and **6**, and 50 μM of compound **4**. Effects of compound **3** on human enzyme could not be assayed because unexpected and systematic precipitation in the reaction medium was observed

Enzyme inhibition assay

Concentration of 100 μM of compound **2** diminished the *Ts*Cu/Zn–SOD activity in 73%; in contrast, the same concentration of this compound did not show any effect on *Hs*Cu/Zn–SOD activity. Compound **3** had an important impact on the *Ts*Cu/Zn–SOD activity, showing 100% inhibition. Unfortunately, effects on human enzyme could not be assayed because unexpected and systematic precipitation in the reaction medium was observed, hence the lacking bar for this assay in Fig. 2. However, the residual activity of *Hs*Cu/Zn–SOD and *Ts*Cu/Zn–SOD at 10 μM of the same compound are 92% and 52%, respectively. The most remarkable results were obtained with compound **4**, which affected *Ts*Cu/Zn–SOD activity in 96% at 50 μM, whereas it had no detectable effect on human Cu/Zn–SOD at the same concentration. With respect to compounds **1**, **5** and **6**, they considerably affected the enzymatic activity of *Ts*Cu/Zn–SOD (49, 48 and 48% of inhibition, respectively) after incubation at 100 μM, but affecting the activity of human enzyme at similar levels; therefore, they can be considered as nonspecific inhibitors. The IC_{50} for compounds **2**, **3** and **4**, (23.9, 10.9 and 25.9 μM, respectively, Fig. 3) confirm that these compounds are good inhibitors, and the last two are also specific for the taenia enzyme. The inactivating effect of **2**, **3** and **4** was concentration dependent. It is noted that the inactivating curves were sigmoidal.

The procedure and results presented here are outstanding due to the identification of novel lead compounds to

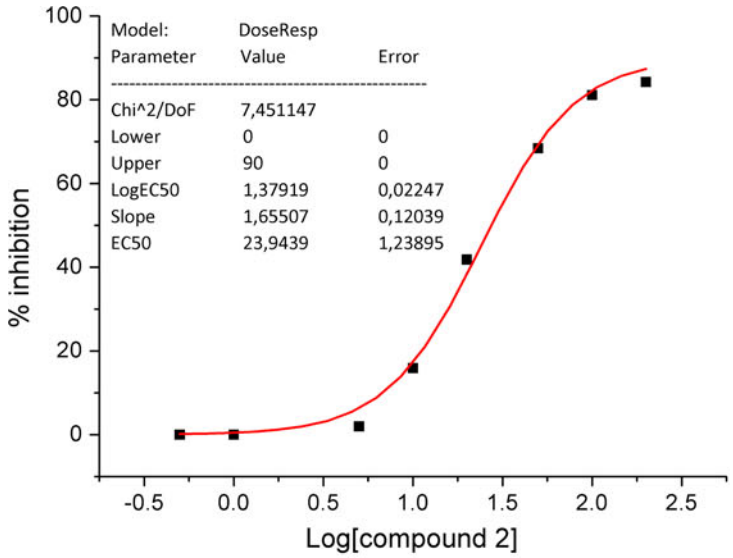

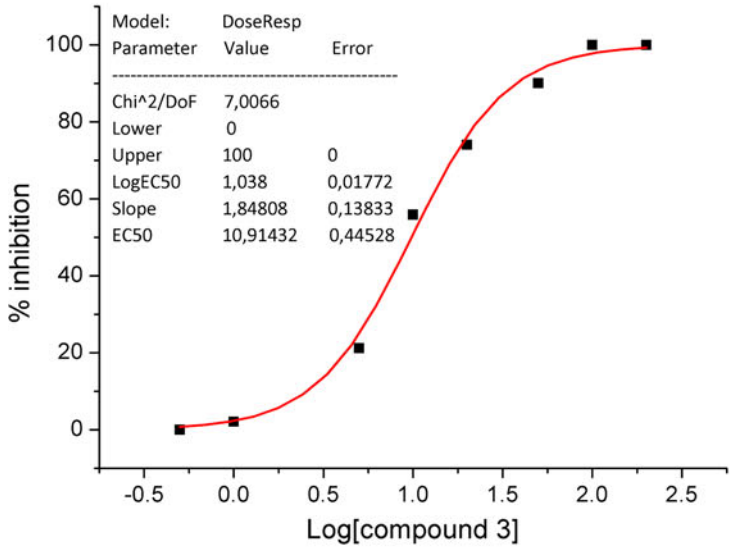

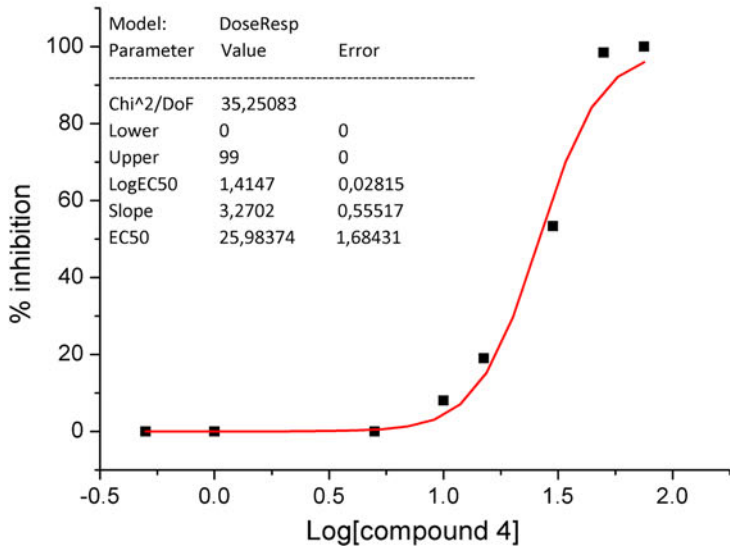

Fig. 3 Curves of inhibition versus inhibitor concentration for compounds **2**, **3** and **4**. See Materials and methods for more details

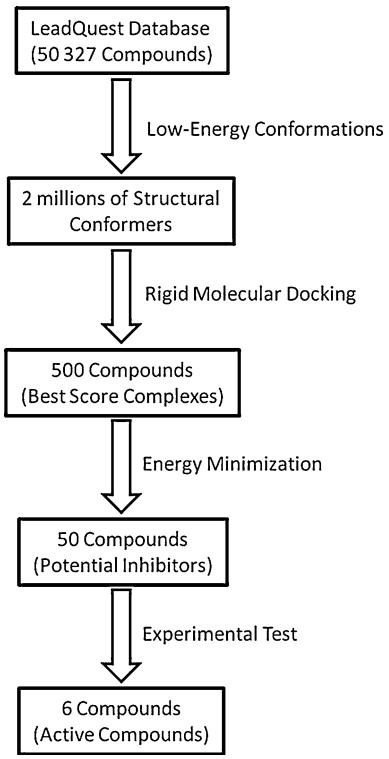

Fig. 4 Flow chart showing the search for lead compounds as inhibitors of *Ts*Cu/Zn–SOD activity by virtual screening followed by experimental assays. *Numbers* represent the amount of molecules selected after each stage

develop more powerful compounds in a future aimed to the design of specific drugs against parasites (Fig. 4).

According to our docking results, compounds **1**–**6** bind near the dimer interface (i.e. sites 1 and/or 2) where the interaction with various conserved and non-conserved residues is strong. For example, compound **4** presented the best inhibitory activity toward *Ts*Cu/Zn–SOD and did not inhibited *Hs*Cu/Zn–SOD at all. Interestingly, we found that all the docked complexes of this compound with docking scores below −7.5 could only be indentified at site 1 (Fig. 5). Compound **4**, docked in its most frequent pose on the *Ts*Cu/Zn–SOD surface, forms a hydrogen bond between the N atom of its pyrimidine ring and the hydroxyl oxygen of the non-conserved Ser*B*108 (Ser108, chain B). Another hydrogen bond was established between the CO group of the carboxylic ethyl ester moiety of the ligand and the NH group of Met*B*1, also a non-conserved residue. Furthermore, the high predicted stability of the complex resulted also from a good shape complementarity, and also from dipole−dipole and van der Waals interactions with nearby residues: the piperazine moiety is located near Met*A*1, Lys*A*2, Leu*A*103, Ser*A*108, Ile*A*110, and Ile*A*148, while the pyrimidine ring is surrounded by Leu*B*103, Thr*B*104 and Ile*B*110. Good binding poses for compounds **2**, **5** and **6** (i.e. docking scores <−7.5) are identified indistinctly in both sites 1 and 2. Compounds **1** and **3** seem to bind exclusively to site 1 as previously described for compound **4**. In Fig. 1, the contact residues (lower than 4.5 Å) in binding site 1 for all active compounds are indicated, and the protein residues which form hydrogen bonds are highlighted. Selectivity might arise from different short and medium distance interactions. Some of the most relevant short-distance contacts include parasite residues: Thr104, and hydrogen bonding to Ser108, Met1, Lys150, Ser151. All these residues in taenia enzyme are different in the human orthologue. Figure 6 shown binding poses of compound **6** in sites 1 and 2 on the surface of *Ts*Cu/Zn–SOD enzyme after docking and the 3-step energy minimization protocol. Schemes of protein–ligand interactions are shown in Figure 1 in Supplementary Material.

It must be considered that docking scores are designed as a fast evaluation of multiple poses of every conformation analyzed from each potential ligand, to select the top scored compounds as an enriched subset of the chemolibrary, and not as an accurate predictor of binding affinity or biological activity. Albeit in some publications certain correlation between IC_{50} and docking scores can be found, it must be considered that for the above reason, a high correlation between docking score and IC_{50} must not be always expected [37].

We found in our case of study that although docking is sometimes seen as an automatic procedure, human intuition to get advantage of robustness and selectivity may still be a good ingredient during the analysis of docking results.

As far as we know, this is the first time that inhibitors have been proposed and tested for this enzyme; specifically, compounds **1**–**6** can be considered as novel inhibitors of *Ts*Cu/Zn–SOD and could constitute a set of starting points to design more powerful inhibitors opening a new way to tackle infections of *T. solium* and other parasites.

Many enzymes and proteins are regulated by their quaternary structure and/or by their association in homo and/or hetero-oligomer complexes. Thus, these protein–protein interactions can be good targets for blocking or modulating protein function therapeutically [38] Eukaryotic Cu/Zn–SOD has a stable β-barrel fold and a dimer assembly, shows diffusion-limited catalysis and electrostatic guidance of their free-radical substrate. Disruption of the quaternary structure appears to decrease the catalytic activity: Banci and coworkers [39, 40] have replaced two hydrophobic residues (Phe50 and Gly91) at the dimer interface of the human enzyme, producing a soluble monomer with a much lower activity (around 10%) than that of the native dimeric enzyme. Using X-ray diffraction [41] as well as NMR techniques [39], these authors observed changes in the conformation of the loop (residues 120–139) responsible for generating the electrostatic potential for driving superoxide anions to the metallic ions

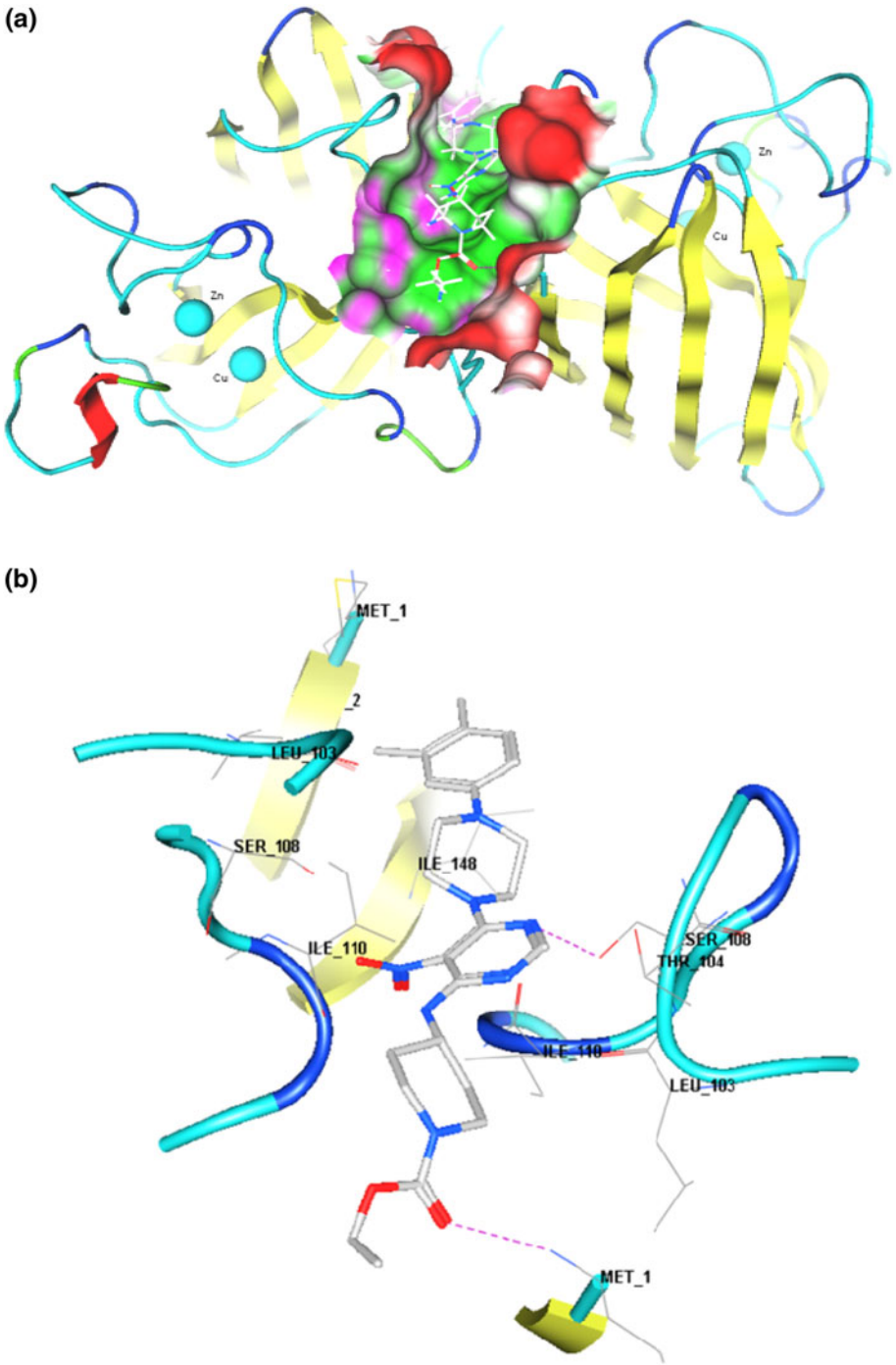

Fig. 5 **a** Binding pose of compound **4** in the *Ts*Cu/Zn–SOD binding site 1 after docking and the 3-step energy minimization procedure. **b** Network of hydrogen bonds (*red dashed lines*) between **4** and the amino acids in the *Ts*Cu/Zn–SOD binding site 1. See description in the text

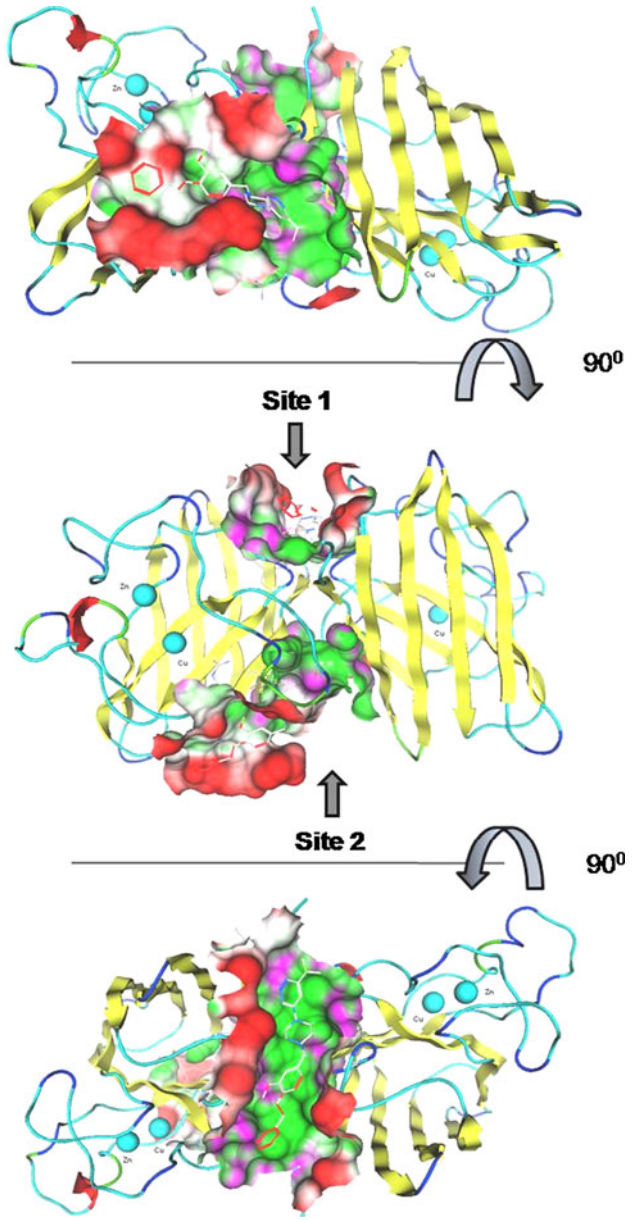

Fig. 6 Binding poses of compound **6** in sites 1 and 2 on the surface of *Ts*Cu/Zn–SOD enzyme after docking and the 3-step energy minimization procedure

at the active site. Also the backbone mobility of the monomeric state was investigated with molecular–dynamics simulations and compared to that of the dimeric species and it was concluded that, as far as motions in the picoseconds to nanoseconds timescale are concerned, the region consisting of residues 131–142 is less mobile in the monomeric mutant than in the dimeric wild-type protein. Structural fluctuations in this region have been suggested to play a role in assisting the superoxide anion in sliding towards the active site [42, 43].

On these bases, we suggest that compounds **1–6** affect the enzyme activity either by disrupting the monomer–monomer interface or by restricting the movements of the loops at each monomer, thus limiting the diffusion of the substrate to the reaction site.

Further studies are being carried out in order to establish the molecular mechanism of the inhibitory action of these compounds.

Conclusion

In summary, six new inhibitors of the *Ts*Cu/Zn–SOD enzymatic activity have been discovered using a methodology developed here which consisted in generating a conformational database from the LeadQuest® database, docking procedures, species selectivity filtering, and finally a proposal of subsequent ligand optimization based on three energy minimization steps over the best protein–ligand complex scores. Three of these compounds showed excellent selectivity to *Ts*Cu/Zn–SOD since they affect the activity of this enzyme at μM range but did not show inhibition against *Hs*Cu/Zn–SOD. Results obtained here are very promising, and now further studies are being carried out to determine the mechanism involved in the inactivation observed against *Ts*Cu/Zn–SOD and *Hs*Cu/Zn–SOD for compounds **1–6**.

Acknowledgments This work was partially suported by Consejo Nacional de Ciencia y Tecnología-México (CONACyT, 105532, 80134-M, ECOS M05-501) and the Dirección General de Asuntos del Personal Académico (DEGAPA, IN 207507-3). P.G.-G. and R.P.-U. also thank CONACyT for graduate studies grants.

References

1. Del Brutto OH, Sotelo J, Roman GC (1998) Neurocysticercosis: a clinical handbook. Swets and Zeitlinger Publisher, Lisse, pp 216–222
2. García HH, González AE, Evans CA, Gilman RH (2003) *Taenia solium* cysticercosis. Lancet 362:547–556
3. Wallin MT, Kurtzke JF (2004) Neurocysticercosis in the United States. Review of an important emerging infection. Neurology 63:1559–1564
4. Bern C, García HH, Evans C, González AE, Verastegui M, Tsang VC, Gilman RH (1999) Magnitude of the disease burden from neurocysticercosis in a developing country. Clin Infect Dis 29:1203–1209
5. Carpio A, Escobar A, Hauser WA (1998) Cysticercosis and epilepsy: a critical review. Epilepsia 39:1025–1040
6. Mafojane NA, Appleton CC, Krecek RC, Michael LM, Willingham AL (2003) The current status of neurocysticercosis in Eastern and Southern Africa. Acta Trop 87:25–33
7. Takayanagui OM, Jardim E (1992) Therapy for neurocysticercosis: comparison between albendazole and praziquantel. Arch Neurol 49:290–294
8. Chong MS, Hawkins CP, Cook GC, Hawkes CH, Kocen RS (1991) A resistant case of neurocysticercosis. Postgrad Med J 67:577–578

9. Köhler P (2001) The biochemical basis of anthelminthic action and resistance. Int J Parasitol 31:336–345
10. Stepek G, Behnke JM, Buttle DJ, Duce IR (2004) Natural plant cysteine proteinases as anthelmintics? Trends Parasitol 20:323–327
11. Fridovich I (1998) Oxygen toxicity: a radical explanation. J Exp Biol 201:1203–1209
12. Vaca-Paniagua F, Torres-Rivera A, Unda-Parra R, Landa A (2008) Taenia solium: Antioxidant metabolism enzymes as target for cestocidal drugs and vaccines. Curr Top Med Chem 8:393–399
13. Birnboim HC, Kanabus-Kaminka M (1985) The production of DNA strands breaks in human leukocytes by superoxide anion may involve a metabolic process. Proc Natl Acad Sci USA 82:6820–6824
14. Henkle-Dührsen K, Kampkötter A (2001) Antioxidant enzyme families in parasitic nematodes. Mol Biochem Parasitol 114:129–142
15. Loverde PT (1998) Do antioxidants play a role in schistosoma host parasite interactions? Parasitol Today 4:284–289
16. Monroy-Ostria A, Monroy-Ostria TJ, Gómez G, Hernández MO (1993) Some studies on experimental infection of golden hamsters with *Taenia solium*. Rev Lat Microbiol 35:91–98
17. Sánchez-Moreno M, León P, Salas-Peregrin JM, Osuna A (1988) Superoxide dismutase in trematodes. Arzneimittelforschung 37:903–905
18. Sánchez-Moreno M, García-Ruiz A, García-Rejón L, Valero A, León P (1989) Superoxide dismutase in cestodes. Isoenzymatic characterization and studies of inhibition by series of benzimidazoles and by pyrimidine derivates of recent synthesis. Drug Res 39:759–761
19. Sánchez-Moreno M, Entrala E, Janssen D, Fernández-Becerra C, Salas-Peregrin JM, Osuna A (1996) Inhibition of superoxide dismutase from *Ascaris suum* by benzimidazols and synthesized pyrimidine and glycine derivatives. Pharmacology 52:61–68
20. Castellanos-González A, Jiménez L, Landa A (2002) Cloning, production and characterization of a recombinant Cu/Zn superoxide dismutase from *Taenia solium*. Int J Parasitol 81:541–546
21. Sanz AM, Gómez-Contreras F, Navarro P, Sánchez-Moreno M, Boutaleb-Charki S, Campuzano J, Pardo M, Osuna A, Cano C, Yunta MJR, Campayo L (2008) Efficient inhibition of iron superoxide dismutase and of growth *Trypanosoma cruzi* by benzo[*g*]phthalazine derivatives functionalized with one or two imidazole rings. J Med Chem 51:1962–1966
22. Temperton NJ, Wilkinson SR, Meyer DJ, Kelly JM (1998) Overexpression of superoxide dismutase in *T. cruzi* results in increased sensitivity to the trypanocidal agents gentian violet and benznidazole. Mol Biochem Parasitol 96:167–176
23. Hernández-Santoyo A, Landa A, González-Mondragón E, Pedraza-Escalona M, Parra-Unda R, Rodríguez-Romero A (2011) Crystal structure of Cu/Zn superoxide dismutase from *Taenia solium* reveals metal-mediated self-assembly. FEBS J (In press)
24. Molecular Operating Environment (MOE). Chemical Computing Group, Inc. CCG, Montreal, Canada. http://www.chemcomp.com . Versions 2005.06 and 2007.09
25. LeadQuest® Compound Library, April 2006, Exelgen, Inc. 1699 South Hanley Road, St. Louis, MO 63144 USA
26. Liang J, Edelsbrunner H, Woodward C (1998) Anatomy of protein pockets and cavities: Measurement of binding site geometry and implications for ligand design. Protein Sci 7:1884–1897
27. Edelsbrunner H Weighted Alpha Shapes. Department of Computer Science, University of Illinois at Urbana-Champaign, Urbana, Illinois 61810
28. This function estimates the enthalpic contribution to the free energy of binding using a linear function: $G = C_{hb}f_{hb} + C_{ion}f_{ion} + C_{mlig}f_{mlig} + C_{hh}f_{hh} + C_{hp}f_{hp} + C_{aa}f_{aa}$, where the f terms fractionally count atomic contacts of specific types and the Cs are coefficients that weight the term contributions to estimate the docking score
29. Wood ER, Truesdale AT, McDonald OB, Yuan D, Hassell A, Dickerson SH, Ellis B, Pennisi C, Horne E, Lackey K, Alligood KJ, Rusnak DW, Gilmer TM, Shewchuk L (2004) A unique structure for epidermal growth factor receptor bound to GW572016 (Lapatinib): relationships among protein conformation, inhibitor off-rate, and receptor activity in tumor cells. Cancer Res 64:6652–6659
30. Kuntz ID (1993) Structure–base strategies for drug design and discovery. Science 33:107–115
31. Trott O, Olson AJ (2010) AutoDock Vina: improving the speed and accuracy of docking with a new scoring function, efficient optimization, and multithreading. J Comput Chem 31:455–461
32. Sanner MF (1999) Python: a programming language for software integration and development. J Mol Graph Model 17:57–61
33. McCord JM, Fridovich I (1969) Superoxide dismutase. An enzymic function for erythrocuprein (hemocuprein). J Biol Chem 244:6049–6055
34. Perola E, Charifson P (2004) Conformational analysis of drug-like molecules bound to proteins: An extensive study of ligand reorganization upon binding. J Med Chem 47:2499–2510
35. Laurie ATR, Jackson RM (2006) Methods for the prediction of protein–ligand binding sites for structure-based drug design and virtual ligand screnning. Curr Protein Pept Sci 7:395–406
36. Molinspiration Property Calculation Service. http://www.molinspiration.com
37. Park MS, Dessal AL, Smrcka AV, Stern HA (2009) Evaluating docking methods for prediction of binding affinities of small molecules to the G protein beta-gamma subunits. J Chem Inf Model 49:437–443
38. Cardinale D, Salo-Ahen OMH, Ferrari S, Ponterini G, Cruciani G, Carosati E, Tochowicz AM, Mangani S, Wade RC, Costi MP (2010) Homodimeric enzymes as drug targets. Curr Med Chem 17:826–846
39. Banci L, Benedetto I, Bertini R, Del Conte M, Piccioli M, Viezzoli MS (1998) Solution structure of reduced monomeric Q133M2 copper, zinc superoxide dismutase. Why is SOD a dimeric enzyme? Biochemistry 37:11780–11791
40. Banci L, Bertini I, Del Conte R, Mangani S, Viezzoli MS, Fadin R (1999) The solution structure of a monomeric reduced form of human copper, zinc superoxide dismutase bearing the same charge as the native protein. J Biol Inorg Chem 4:795–803
41. Ferraroni M, Rypniewski W, Wilson KS, Viezzoli MS, Banci L, Bertini I, Mangani S (1999) The crystal structure of the monomeric human SOD mutant F50/G51E/E133Q at atomic resolution. The enzyme mechanism revisited. J Mol Biol 288:413–426
42. Luty BA, El Amrani S, McCammon JA (1993) Simulation of the bimolecular reaction between superoxide and superoxide dismutase: synthesis of the encounter and reaction steps. J Am Chem Soc 115:11874–11877
43. Banci L, Bertini I, Cramaro F, Del Conte R, Rosato A, Viezzoli MS (2000) Backbone dynamics of human Cu, Zn superoxide dismustase and of its monomeric F50/EG51E/E133Q mutant: The influence of dimerization on mobility and function. Biochemistry 39:9108–9118